Experimental demonstration of a hybrid plasmonic transverse electric pass polarizer for a silicon-on-insulator platform

X. Sun,* M. Z. Alam, S. J. Wagner, J. S. Aitchison, and M. Mojahedi

Edward S. Rogers Sr. Department of Electrical and Computer Engineering, University of Toronto, Toronto, Ontario M5S 3G4, Canada

**Corresponding author: xiaoxiao.sun@mail.utoronto.ca*

Received August 31, 2012; revised October 17, 2012; accepted October 17, 2012; posted October 17, 2012 (Doc. ID 175283); published November 16, 2012

We experimentally demonstrate a transverse electric (TE)-pass polarizer using the recently proposed hybrid plasmonic waveguide. The device consists of a silicon film separated from a chromium layer by a silica spacer. The device was characterized using a tunable laser in the 1.52–1.58 μm wavelength range. For a 30 μm long polarizer, the extinction ratio in this wavelength range varies from 23 to 28 dB and the insertion loss for the TE mode is 2–3 dB. The device is compact; its fabrication is completely compatible with silicon-on-insulator technology, and its performance compares favorably against previously reported silicon-based integrated optic TE-pass polarizers.

OCIS codes: 130.3120, 240.6680.

Control of the polarization state of light is essential for many integrated optics applications [1]. This is especially true for high-index contrast waveguides, such as those implemented on the silicon-on-insulator (SOI) platform. The high index of silicon makes SOI waveguides highly polarization dependent. Thus, the transverse electric (TE) and transverse magnetic (TM) modes behave differently in such waveguides, and the absence of polarization control may disrupt the proper operation of the integrated chip. One common approach to solve this problem is to use a polarizer to extinguish the unwanted polarization state. Several different types of SOI-compatible TE-pass polarizers have been proposed, including metal clad waveguides [2,3], shallowly etched waveguides [4], and gap plasmon waveguides [5]. These devices are sensitive to fabrication imperfection, are long, or have significant insertion loss for the TE mode. To implement complex optical circuits with many integrated components and to increase the integration density, an experimental demonstration of a compact, broadband, and SOI-compatible TE-pass polarizer with better solution for polarization control is required.

Recently, we have proposed a hybrid plasmonic waveguide (HPWG) consisting of a metal plane separated from a high-index medium by a low-index spacer [6,7]. The guide is compact, is compatible with SOI technology, and provides a better compromise between loss and confinement than previously reported plasmonic waveguides. Many different kinds of HPWG have been proposed [6–10] and various applications have been suggested, including biosensors [11] and nonlinear optical devices [12]. In our previous work, we suggested that HPWG could be used to implement a compact, broadband TE-pass polarizer that could provide high extinction ratio and low insertion loss for the TE mode [13]. In this Letter, we report the experimental demonstration of such a device.

Figure 1(a) shows a schematic of the TE-pass polarizer. It consists of an HPWG section [Fig. 1(b)] between two silicon waveguides [Fig. 1(c)]. The low-loss input and output silicon waveguides are used to guide the light over large distances into and out of the HPWG section, and the HPWG section is used to extinguish the TM mode. We have designed the device to achieve a high extinction ratio using a short HPWG section, as reported in our previous work [13]. In addition to the theoretical considerations described in our previous work, in this Letter, we also have considered the fabrication simplicity and the smooth propagation of the TE mode in the whole device. Moreover, we have eliminated the partial etching of the silicon, which avoids creating roughness on the silicon top surface and improves the coupling efficiency between different sections. In particular, a smooth transition between different sections for the desired TE mode is achieved, as discussed later.

The electric-field intensity profiles for TE and TM modes for the HPWG, obtained by using the finite difference method, are shown in Figs. 2(a) and 2(b), respectively. Similar to dielectric waveguides, in an HPWG, the electric field for the TE mode is concentrated in the high index region (i.e., silicon core). The TM mode, on the other hand, is a hybrid mode and the electric field is concentrated in the silica between the metal and silicon. Because the TM mode is adjacent to the metal, the propagation loss for the TM mode in the HPWG is always larger than that for the TE mode. Based on this principle, a TE-pass polarizer can be implemented using the HPWG.

We optimized the design of the TE-pass polarizer using the finite difference time domain (FDTD) software from Lumerical Solutions. A nonuniform mesh with a 5 nm

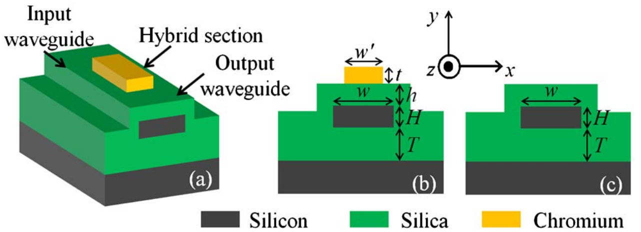

Fig. 1. (Color online) (a) Three-dimensional schematic of the HPWG TE-pass polarizer. (b) Cross section of the HPWG. (c) Cross section of the input-output silicon nano waveguide.

0146-9592/12/234814-03$15.00/0

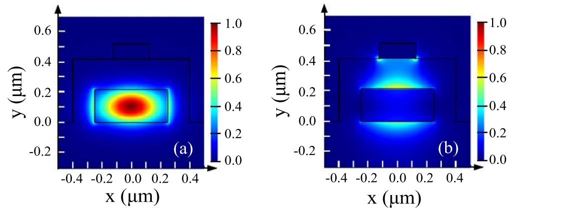

Fig. 2. (Color online) Electric field intensity profiles at 1.55 μm for the (a) TE and (b) TM modes of the HPWG section for $H = 220$ nm, $T = 3$ μm, $w = 500$ nm, $w' = 250$ nm, $h = 200$ nm, and $t = 100$ nm. For the definition of the variables, see Fig. 1.

mesh size at the metal-dielectric interface and relatively larger mesh elsewhere in the computational volume were used. The final dimensions, illustrated in Fig. 1, are $H = 220$ nm, $T = 3$ μm, $w = 500$ nm, $w' = 250$ nm, $h = 200$ nm, and $t = 100$ nm. These dimensions ensure single-mode guiding, high coupling efficiency between different sections, and high extinction ratio. Additionally, the design is tolerant to possible variations of the device dimensions. Because the dimensions of the HPWG are exactly the same as the input-output waveguides (except for a metal cap), the coupling losses between different sections are low. For the TE mode, we have ensured that the mode shape, position, and refractive index match well between sections, and thus the reflection and scattering losses between different sections have been suppressed. At 1.55 μm wavelength, the coupling efficiency of the TE mode between sections is more than 99%, which ensures a smooth transition for the TE mode. Conversely, for the TM mode—because of the influence of the chromium—there is some shape and effective index mismatch; thus, the coupling efficiency between sections is approximately 88% at each interface, and some power is reflected and scattered. Figure 3 (black square line) shows the device insertion losses (including coupling and propagation losses) obtained from the full-wave FDTD simulation for a 30 μm long HPWG TE-pass polarizer inserted between two silicon nano waveguides. It shows a high extinction ratio and a low device insertion loss for the TE mode over a bandwidth of 150 nm.

During fabrication, precise control of the width of the silicon nano waveguide is not an easy task because of the undercut in etching; however, deviation under tens of nanometer is achievable. We have investigated the performance of the polarizer for $w = 500\ \text{nm} \pm 50$ nm and have plotted the results in Figs. 3(a) and 3(b). Smaller w results in higher losses for both modes because less power is confined in the silicon region and more power resides in the regions adjacent to the chromium; thus, the modes are more susceptible to metal absorption. The ripples present in the TM-mode insertion loss spectrum are the result of the reflection and the scattering because of the mode mismatch between different sections. These results indicate that the proposed device can provide a large insertion loss for the TM mode while maintaining a low insertion loss for the TE mode over a range of dimensions.

The TE-pass polarizer was implemented on an SOI substrate consisting of a 220 nm thick silicon device layer on a 3 μm buried oxide layer. In the first step, a positive-electron beam resist ZEP520 was spun on the substrate and patterned using electron beam lithography. This was followed by reactive ion etching (RIE) to define the silicon nano waveguides. A 200 nm silica layer was then deposited over the sample using plasma-enhanced chemical vapor deposition. Electron beam lithography was used again to define the HPWG section. The sample was then covered with chromium using a thermal evaporation process followed by a lift-off process to complete the fabrication.

A number of TE-pass polarizers of various lengths (between 20 and 40 μm) were fabricated on the same chip. In addition, a number of reference channels also were fabricated. The reference channels are identical to the TE-pass polarizer branches with the exception that they have no HPWG sections. Figures 4(a) and 4(b) show the scanning electron microscopy (SEM) images of the top view and end facet of the HPWG section, respectively. The chromium section is 250 nm wide and 150 nm thick. It is located almost at the middle of the HPWG section with a small offset (25 nm), which confirms the good alignment achieved in our fabrication. The RIE process produced a trapezoidal shape for the silicon nano waveguide with the width of the trapezoid varying from 580 nm at the bottom to 420 nm at the top. From the simulation results, presented later in this Letter, we shall see that this deviation from the original design does not significantly affect the device performance.

We used an end-fire scheme to test the fabricated devices. Power from a continuous wave tunable InGaAsP laser was coupled to free space from a single-mode fiber using a fiber-to-free-space coupler. The polarization of the incident light was controlled using a combination of half wave plate and polarizing beam cube. The sample was mounted on a rig and two 40× microscope objectives were used to couple the light in and out of the sample. An infrared camera was used at the output to ensure that

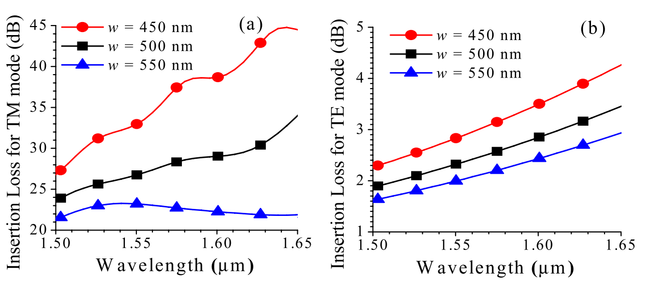

Fig. 3. (Color online) Variation of device insertion loss of the (a) TM mode and (b) TE mode with silicon width (w) of a 30 μm long HPWG. $H = 220$ nm, $T = 3$ μm, $w' = 250$ nm, $h = 200$ nm, $t = 100$ nm.

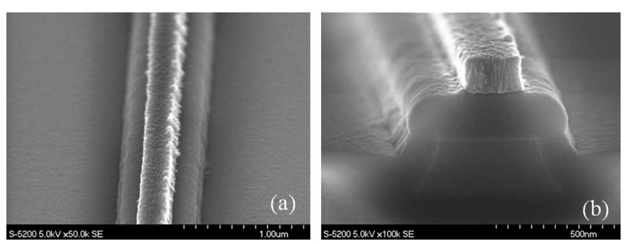

Fig. 4. SEM images of the HPWG section (a) top and (b) end view.

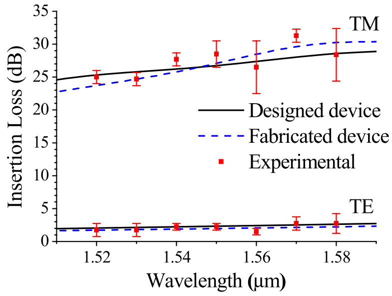

Fig. 5. (Color online) Device insertion losses of the TE and TM modes for a 30 μm long HPWG TE-pass polarizer.

light was coupled properly to only one waveguide at a time. The power output of the TE-pass polarizer waveguide was compared with that of the reference waveguide to measure the device insertion loss.

The measured device insertion losses for both TE and TM modes are shown in Fig. 5 (markers) over a wavelength range of 1.52–1.58 μm. The insertion loss for the TM mode varies from 25 to 31 dB and the insertion loss for the TE mode varies from 2–3 dB, which results in an extinction ratio ranging from 23 to 28 dB. We compared several fabricated TE-pass polarizers and reference waveguides; the performance is slightly different among them. The error bars on the plot reflect such a difference. Although the device is expected to work well beyond the 1.52–1.58 μm wavelength range, the finite bandwidth of our tunable laser precluded measurement over a wider range. In addition to the experimentally measured losses, simulated losses for the TM and TE modes of the designed polarizer (with rectangular cross section) are shown in Fig. 5 (solid line). Figure 5 also displays the simulated losses for the fabricated device with trapezoidal cross section and off-center chromium layer (dashed lines). Simulation results for the designed and fabricated device indicate that device deviations from its design parameters have little effect on its performance (less than 3 dB for the TM mode and less than 1 dB for the TE mode).

From Fig. 5, we observe that the experimental results agree well with the predictions from simulations. The slight discrepancy between the simulations and experimental results is not unexpected. For our simulations, we have taken the material properties of the chromium from Palik [14]. The permittivity of the chromium, especially the imaginary part of the permittivity, can vary depending on the growth conditions, which will result in some discrepancy. Moreover, in our simulations, we have neglected the losses because of the scattering from surface roughness. When comparing the TE-pass polarizer with the reference waveguides, the scattering losses from the silicon nano waveguides are not an issue because both have similar scattering losses, but there are additional scattering losses between the chromium and silica in the hybrid section. The precision of the measurement also affects the experimental results; especially because the output power of the TM mode is very small, making the recoding of the data for this mode quite sensitive to the background noise from the substrate. All these factors will contribute to the discrepancy between the simulations and measurements for the polarizer, but as we can see by comparing the plots in Fig. 5, the agreement between the measurement and simulation is still very good.

We predict that the HPWG TE-pass polarizer can outperform previously proposed SOI-compatible TE-pass polarizers in Alam *et al.* [13]. Although many different types of TE-pass polarizers have been investigated in the past, only a few experimental demonstrations of SOI-compatible TE-pass polarizers have been completed [3,4]. A silicon rib waveguide coated with aluminum can act as a TE-pass polarizer [3], but the device length is more than 1 mm and the extinction ratio achieved is relatively low ($<$20 dB). Shallow-etched ridge waveguide TE-pass polarizers reported in [4] are simple to fabricate, and the insertion loss of the TE and TM modes achieved for the device are comparable to that of our current work, but the device is 1 mm long. Here, we have achieved an extinction ratio from 23 to 28 dB and a moderate loss for the TE mode for a device length of only 30 μm.

In conclusion, we have fabricated a hybrid plasmonic TE-pass polarizer and measured its performance. The experimental results validate the predictions of our simulation. The device is compact, has low insertion loss, and provides a possibility to shorten the integrated optical circuits where TE-pass polarization is needed.

This work was supported by the Natural Science and Engineering Research Council (NSERC) of Canada under grant no. 480586 and Biopsys Network under grant no. 486537. We would like to acknowledge CMC Microsystems in preparing the devices described in this work.

References

1. D. Dai, J. Bauters, and J. E. Bowers, Light Sci. Appl. **1**, e1 (2012).
2. V. K. Sharma, A. Kumar, and A. Kapoor, Opt. Commun. **284**, 1815 (2011).
3. G. R. Bhatt and B. K. Das, Opt. Commun. **285**, 2067 (2012).
4. D. Dai, Z. Wang, N. Julian, and J. E. Bowers, Opt. Express **18**, 27404 (2010).
5. I. Avrutsky, IEEE J. Sel. Topics Quantum Electron. **14**, 1509 (2008).
6. M. Z. Alam, J. Meier, J. S. Aitchison, and M. Mojahedi, in *Conference on Lasers and Electro-optics (CLEO)/ Quantum Electronics and Laser Science Conference (QELS)*, OSA Tech. Digest (OSA,2007), paper JThD112.
7. M. Z. Alam, J. Meier, J. S. Aitchison, and M. Mojahedi, Opt. Express **18**, 12971 (2010).
8. R. F. Oulton, V. J. Sorger, D. A. Genov, D. F. P. Pile, and X. Zhang, Nat. Photonics **2**, 496 (2008).
9. D. Dai and S. He, Opt. Express **17**, 16646 (2009).
10. X. Zuo and Z. Sun, Opt. Lett. **36**, 2946 (2011).
11. F. Bahrami, M. Z. Alam, J. S. Aitchison, and M. Mojahedi, "Dual polarization measurements in the hybrid plasmonic biosensors," Plasmonics, online first, doi: 10.1007/s11468-012-9411-z (2012).
12. F. F. Lu, T. Li, X. P. Hu, Q. Q. Cheng, S. N. Zhu, and Y. Y. Zhu, Opt. Lett. **36**, 3371 (2011).
13. M. Z. Alam, J. Stewart Aitchison, and M. Mojahedi, Opt. Lett. **37**, 55 (2012).
14. E. D. Palik, *Handbook of Optical Constants of Solids* (Academic, 1985).